

Article

Fed-Batch Control and Visualization of Monomer Sequences of Individual ICAR ATRP Gradient Copolymer Chains

Dagmar R. D'hooge, Paul H. M. Van Steenberge, Marie-Françoise Reyniers * and Guy B. Marin

Laboratory for Chemical Technology (LCT), Ghent University, Technologiepark 914, B-9052 Zwijnaarde (Gent), Belgium; E-Mails: dagmar.dhooge@ugent.be (D.R.D.); paul.vansteenberge@ugent.be (P.H.M.V.S.); guy.marin@ugent.be (G.B.M.)

* Author to whom correspondence should be addressed; E-Mail: mariefrancoise.reyniers@ugent.be; Tel.: +32-9-331-1754; Fax: +32-9-331-1759.

Received: 28 February 2014; in revised form: 31 March 2014 / Accepted: 2 April 2014 /

Published: 10 April 2014

Abstract: Based on kinetic Monte Carlo simulations of the monomer sequences of a representative number of copolymer chains ($\approx 150,000$), optimal synthesis procedures for linear gradient copolymers are proposed, using bulk Initiators for Continuous Activator Regeneration Atom Transfer Radical Polymerization (ICAR ATRP). Methyl methacrylate and *n*-butyl acrylate are considered as comonomers with $\text{CuBr}_2/\text{PMDETA}$ (*N,N,N',N'',N'''*-pentamethyldiethylenetriamine) as deactivator at 80 °C. The linear gradient quality is determined *in silico* using the recently introduced gradient deviation ($\langle\text{GD}\rangle$) polymer property. Careful selection or fed-batch addition of the conventional radical initiator I_2 allows a reduction of the polymerization time with *ca.* a factor 2 compared to the corresponding batch case, while preserving control over polymer properties ($\langle\text{GD}\rangle \approx 0.30$; dispersity ≈ 1.1). Fed-batch addition of not only I_2 , but also comonomer and deactivator (50 ppm) under starved conditions yields a $\langle\text{GD}\rangle$ below 0.25 and, hence, an excellent linear gradient quality for the dormant polymer molecules, albeit at the expense of an increase of the overall polymerization time. The excellent control is confirmed by the visualization of the monomer sequences of *ca.* 1000 copolymer chains.

Keywords: ICAR ATRP; kinetic Monte Carlo modeling; optimization; copolymer composition; gradient deviation; starved-feed conditions

List of symbols:

a	activation
ATRP	atom transfer radical polymerization
C_{I2}	concentration of conventional radical initiator ($\text{mol}\cdot\text{L}^{-1}$)
CRP	controlled radical polymerization (also known as RDRP)
da	deactivation
dis	dissociation
EGF	end-group functionality (denoted as X)
i, j	chain length
I	conventional radical initiator fragment
I_2	conventional radical initiator
ICAR	initiators for continuous activator regeneration
<GD>	(average) linear gradient deviation (-)
$F_{1,\text{inst}}$	instantaneous copolymer composition (-)
f	efficiency (-)
f_1	monomer feed composition with respect to <i>n</i> BuA; molar fraction of <i>n</i> BuA in the reaction mixture (-)
kMC	kinetic Monte Carlo
M	monomer
$[M_i]$	concentration of comonomer i ($i = 1: n\text{BuA}; i = 2: \text{MMA}$)
MMA	methyl methacrylate
$M_i^n L_y X$	activator
$M_i^{n+1} L_y X_2$	deactivator
<i>n</i> BuA	<i>n</i> -butyl acrylate
p	propagation
RAFT-CLD-T	reversible addition fragmentation chain transfer polymerization-chain length dependent-termination
RDRP	reversible deactivation radical polymerization (also known as CRP)
R_0	ATRP initiator radical
R_0X	ATRP initiator
R_i	macroradical
R_iX	dormant macrospecies
r_i	reactivity ratio of monomer i (-)
$t(c/d)$	termination by recombination/disproportionation
TCL	targeted chain length (for complete monomer conversion)
x_{overall}	overall monomer conversion (with respect to <i>batch</i> amount)
z	number
0	related to ATRP initiator

1. Introduction

During the last decades, the design of well-tailored polymers molecules with predetermined number average chain length, high end-group functionality (EGF), controlled topology and low dispersity has been the topic of many research activities [1–14]. These advanced macromolecular architectures are typically acquired via controlled radical polymerization (CRP), which is also known as reversible deactivation radical polymerization (RDRP). In contrast to conventional free radical polymerization (FRP), in CRP, termination reactions are suppressed, due to a dominant role of deactivation reactions, which temporarily transforms radicals in dormant species via inclusion of EGF.

Deactivation of radicals is possible thanks to the presence of a mediating agent, such as a transition metal complex, a nitroxide or a degenerative chain transfer agent. For sufficiently high deactivation rates, per activation-growth-deactivation cycle, only a limited number of monomer units are incorporated and, hence, a concurrent growth of dormant species takes place. For a fast CRP initiation, all dormant species possess after complete monomer depletion ideally a chain length equal to the initial molar ratio of monomer to “CRP initiator”, *i.e.*, the targeted chain length (TCL).

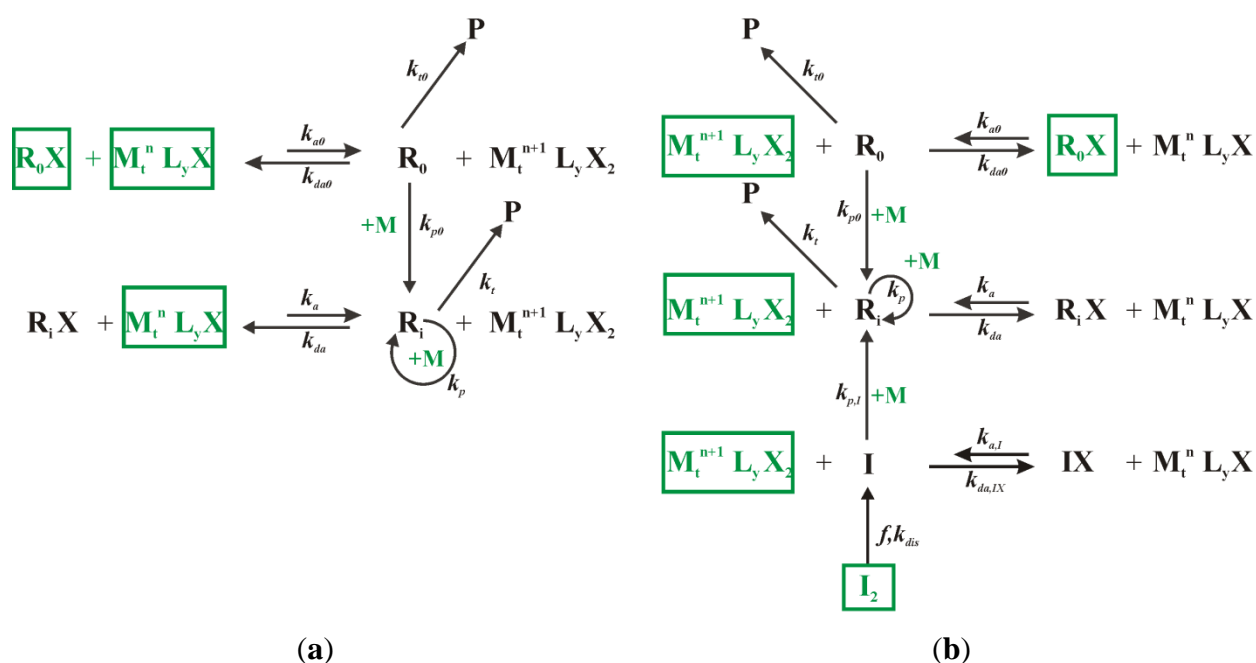
In Scheme 1a, the principle of CRP is illustrated using atom transfer radical polymerization (ATRP) as model CRP technique [3]. In this technique, mostly a Cu based ATRP catalyst is employed as mediating agent, which increases its oxidation state with one unit when participating in activation of dormant species. The latter species are capped with a (pseudo-)halogen atom X as EGF. A persistent radical effect [15] takes place if the ATRP is started in the absence of deactivator, *i.e.*, only activator is initially present. Due to termination, an excess of persistent deactivator species is created, resulting in an increased relative importance of the deactivation rate, leading in turn to control over the ATRP at the expense of a reduction in the polymerization rate.

Unfortunately in these “normal” or original ATRP processes a high catalyst amount (>1000 ppm; with respect to monomer; molar) is required to guarantee both control over chain length and a reasonable polymerization rate [16]. Additionally, the activator is oxygen sensitive implying stringent experimental procedures with respect to oxygen removal and the high ATRP catalyst amounts lead to intensive purification processes. Hence, more recently modified ATRP techniques have been developed in which a low ATRP catalyst amount is used and activator is (re)generated from the oxygen insensitive deactivator through an external source, *e.g.*, an electrode or a reducing agent) [11,16–21]. With these modified techniques, an ATRP catalyst level of *ca.* 50 ppm could be obtained increasing the industrial potential of the ATRP technique [11].

One of the most important modified ATRP techniques is initiators for continuous activators regeneration (ICAR) ATRP, the CRP technique studied in this work. In this technique, as illustrated in Scheme 1b, the activator is (re)generated by a redox reaction of deactivator molecules and oligomeric species originating from conventional radical initiator fragments. However, well-defined polymer products only result after careful selection of the ATRP catalyst and polymerization conditions. Originally, Matyjaszewski *et al.* [18] introduced ICAR ATRP for the controlled synthesis of well-defined poly(methyl methacrylate) and polystyrene using Cu based ATRP catalysts. Later on, using a deterministic modeling approach, D’hooge *et al.* [22] demonstrated that well-defined ICAR ATRP homopolymers can only be obtained in case a sufficiently low conventional radical initiator concentration and a sufficiently high deactivator concentration are considered, since otherwise

FRP-like behavior is observed. For less active catalysts, single or multiple discrete addition(s) of conventional radical initiator can be required to ensure a high conversion. More recently, ICAR ATRP has been also successfully applied with ATRP catalysts made of other transition metals than Cu [23] and in water [21].

Scheme 1. (a) Principle of controlled radical polymerization (CRP) illustrated for “normal” atom transfer radical polymerization (ATRP). (b) Principle of initiators for continuous activator regeneration (ICAR) ATRP; k_a , k_{da} , k_{dis} , k_p and k_t : rate coefficients for activation, deactivation, dissociation, propagation and termination; subscript 0: ATRP initiator; subscript i : macrospecies; subscript I : related to the conventional initiator I_2 ; f : conventional radical initiator efficiency; starting compounds marked in green and boxed (except monomer); activator: $M_t^n L_y X$; deactivator: $M_t^{n+1} L_y X_2$.



For block copolymer synthesis, this high sensitivity of the control over polymer properties to a variation in ICAR ATRP conditions was confirmed by Toloza Porras *et al.* [24], who compared one- and two-pot procedures considering styrene and isobornyl acrylate as comonomers. In particular, these authors illustrated that the order of monomer addition is crucial and the use of a step-wise temperature profile is most suited to improve the block quality. The latter polymer property was assessed by the calculation of a block deviation ($\langle BD \rangle$) value, which is based on the explicit kinetic Monte Carlo (kMC) simulation of the monomer sequences of a representative number of copolymer chains.

In this work, kMC simulations are used to further optimize ICAR ATRP copolymerization processes focusing on a second important class of copolymers, *i.e.*, linear gradient copolymers, in which a gradual transition of one comonomer to another comonomer type along the polymer backbones is targeted. It can be expected that control over monomer sequences for such copolymers is even more critical compared to the major controlling challenges faced in block copolymer synthesis, *i.e.*, an effective chain re-initiation and the suppression of the formation of homopolymer chains upon addition of the second comonomer.

In contrast, for linear gradient copolymer synthesis, along the whole process chain re-initiation is relevant, increasing the modeling complexity for instantaneous copolymer composition control.

To obtain gradient monomer sequences in controlled fashion, the use of fed-batch addition of conventional radical initiator, comonomer and deactivator is explored under isothermal conditions, considering methyl methacrylate (MMA) and *n*-butyl acrylate (*n*BuA) as comonomers. The latter comonomers are selected to benefit from the inherent tendency of secondary radical species to be converted into tertiary species. It is shown that an overall Cu level of 50 ppm is required to allow for controlled synthesis of ICAR ATRP linear gradient copolymers and that *in silico* based continuous addition of conventional radical initiator allows to compensate successfully for the negative effect of termination reactions on the ICAR ATRP process. Alternatively, a conventional radical initiator with a sufficiently high half-life time can be used. The highest gradient quality is obtained via a multi-component fed-batch procedure with respect to conventional radical initiator, monomer and deactivator.

2. Kinetic Model

The ICAR ATRP copolymerization of methyl methacrylate (MMA) and *n*-butyl acrylate (*n*BuA) aiming at well-defined gradient copolymers is studied, considering the reaction scheme given in Table 1. The corresponding reference system consists of Cu(I)Br/PMDETA (*N,N,N',N'',N''*-pentamethyldiethylenetriamine) as ATRP catalyst, methyl 2-bromopropionate (MBP) as ATRP initiator (R_0X), and 2,2'-azobis(2-methylpropionitrile) (AIBN) as conventional radical initiator. For simplicity, a terminal model is used, *i.e.*, the reactivity is assumed to be solely determined by the last monomer unit. In general, it can be expected that a penultimate model is more suited, as frequently only the overall copolymer composition is accurately described [25].

In Table 1, the values of the intrinsic rate coefficients are also provided at 80 °C, the polymerization temperature selected in this work. Except for reactions involving conventional radical initiator fragments, these intrinsic parameters are taken from a previous kinetic study on the related “normal” ATRP system [26]. For simplicity, a constant conventional radical initiator efficiency of 0.70 [22] is used and the activation/deactivation kinetic parameters related to the conventional radical initiator are taken equal to those of the secondary species. As indicated in a recent study on ICAR ATRP of styrene, it can be expected that these parameters have a very limited effect on the overall polymerization rate and control over polymer properties [27], justifying the previous assumption.

Diffusional limitations on termination are accounted for by the calculation of chain length and conversion dependent apparent rate coefficients. The related parameters are taken from Van Steenberge *et al.* [25] and are based on measurements via the RAFT-CLD-T (reversible addition fragmentation chain transfer polymerization-chain length dependent-termination) technique [28,29]. For simplicity, diffusional limitations on the activation/deactivation process are neglected, since they are typically only relevant at high conversions and for bulky mediating agents [30].

Table 1. Overview of reaction steps for copolymerization of *n*BuA (1) and methyl methacrylate (MMA) (2) under ICAR ATRP conditions and corresponding intrinsic parameters at 80 °C (reference system); *f* = 0.7; equal (de)activation rate coefficients for *I* and secondary species: limited effect on results [27].

Reaction	Equation	k_{chem} (80 °C) ((L·mol ⁻¹)·s ⁻¹)	Ref.
Dissociation	$I_2 \xrightarrow{f^{\text{chem}}k_{\text{dis}}^{\text{chem}}} 2I$	1.5×10^{-4}	[31]
	$I + M_1 \xrightarrow{k_{p11}^{\text{chem}}} R_{1,1}$	5.0×10^4	[27]
	$I + M_2 \xrightarrow{k_{p12}^{\text{chem}}} R_{1,2}$	1.5×10^5	[27]
Propagation	$R_0 + M_1 \xrightarrow{k_{p01}^{\text{chem}}} R_{1,1}$	5.0×10^4	[26]
	$R_0 + M_2 \xrightarrow{k_{p02}^{\text{chem}}} R_{1,2}$	1.5×10^5	[26]
	$R_{i,1} + M_1 \xrightarrow{k_{p11}^{\text{chem}}} R_{i+1,1}$	5.0×10^4	[26]
	$R_{i,1} + M_2 \xrightarrow{k_{p12}^{\text{chem}}} R_{i+1,2}$	1.5×10^5	[26]
	$R_{i,2} + M_1 \xrightarrow{k_{p21}^{\text{chem}}} R_{i+1,1}$	4.3×10^2	[26]
	$R_{i,2} + M_2 \xrightarrow{k_{p22}^{\text{chem}}} R_{i+1,2}$	1.3×10^3	[26]
	$M_t^n X/L + IX \xrightarrow{k_{a,IX}^{\text{chem}}} M_t^{n+1} X_2/L + I$	1.0	[27]
Activation	$M_t^n X/L + R_0 X \xrightarrow{k_{a0}^{\text{chem}}} M_t^{n+1} X_2/L + R_0$	1.0	[26]
	$M_t^n X/L + R_{i,1} X \xrightarrow{k_{a1}^{\text{chem}}} M_t^{n+1} X_2/L + R_{i,1}$	1.0	[26]
	$M_t^n X/L + R_{i,2} X \xrightarrow{k_{a2}^{\text{chem}}} M_t^{n+1} X_2/L + R_{i,2}$	10.0	[26]
	$M_t^{n+1} X_2/L + I \xrightarrow{k_{da,I}^{\text{chem}}} M_t^n X/L + IX$	1.0×10^7	[27]
Deactivation	$M_t^{n+1} X_2/L + R_0 \xrightarrow{k_{da0}^{\text{chem}}} M_t^n X/L + R_0$	1.0×10^7	[26]
	$M_t^{n+1} X_2/L + R_{i,1} \xrightarrow{k_{da}^{\text{chem}}} M_t^n X/L + R_{i,1} X$	1.0×10^7	[26]
	$M_t^{n+1} X_2/L + R_{i,2} \xrightarrow{k_{da}^{\text{chem}}} M_t^n X/L + R_{i,2} X$	1.0×10^7	[26]
	$R_0 + R_0 \xrightarrow{k_{tc,00}^{\text{chem}}} R_0 R_0$		
Termination	$R_0 + R_{i,1} \xrightarrow{k_{tc,0i1}^{\text{chem}}} P_i$		
	$R_0 + R_{i,2} \xrightarrow{k_{tc,0i2}^{\text{chem}}} P_i$		
	$R_{i,1} + R_{j,1} \xrightarrow{k_{tc,ij,11}^{\text{chem}}} P_{i+j}$		
	$R_{i,1} + R_{j,2} \xrightarrow{k_{tc,ij,12}^{\text{chem}}} P_{i+j}$		
	$R_0 + R_{i,2} \xrightarrow{k_{td,02}^{\text{chem}}} P_i$		
	$R_{i,2} + R_{j,2} \xrightarrow{k_{td,ij,22}^{\text{chem}}} P_{i+j}$		
	$R_{i,1} + R_{j,2} \xrightarrow{k_{td,ij,12}^{\text{chem}}} P_{i+j}$		

RAFT-CLD-T apparent kinetic parameters to account for diffusional limitations on termination; no intrinsic parameters needed; R_0 treated as $R_{1,1}$ [28,29].

The simulation results are obtained via an explicit kMC modeling approach, in which the monomer sequences of individual polymer chains are tracked. Importantly, the sample size is sufficiently high to ensure an accurate simulation of the ICAR ATRP kinetics, *i.e.*, convergence testing is performed. To assess the gradient quality of the obtained polymers, the recently introduced $\langle \text{GD} \rangle$ (GD: gradient deviation) polymer property, as introduced by Van Steenberge *et al.* [26], is calculated *in silico*, in case the number average chain length is sufficiently high (>10), as for low average chain lengths (≤ 10) no true gradient behavior can be mimicked. In this $\langle \text{GD} \rangle$ calculation, first for each copolymer chain in a representative kinetic Monte Carlo sample, the individual monomer sequences are compared with those of the corresponding “perfect” linear gradient chain possessing the same chain length. Next, normalization with respect to chain length is performed leading to an individual GD value for each copolymer chain considered, *i.e.*, a distribution of macromolecules with respect to their GD results. In a final step, for easy interpretation, $\langle \text{GD} \rangle$ is obtained by calculating the mean of the GD distribution while performing a rescaling between 0 and 1. For example, for a “perfect” linear gradient copolymer, a $\langle \text{GD} \rangle$ value of 0 is obtained, whereas a maximal value of 1 results for a homopolymer. For $\langle \text{GD} \rangle$ values below 0.25, the gradient quality can be seen as high [26].

It should be stressed that a small number of chains, which strongly deviate from the targeted linear gradient microstructure, can already result in a significant higher $\langle \text{GD} \rangle$ value, explaining this relatively high value of 0.25 as a threshold for the linear gradient quality. Furthermore, in the present work, the $\langle \text{GD} \rangle$ value is calculated without accounting for possible losses of low-quality oligomeric chains upon polymer isolation. For more details on the mathematical aspects of the applied kMC modeling approach, the reader is referred to Van Steenberge *et al.* [26,32,34].

3. Results and Discussion

In this section, first the batch bulk ICAR ATRP of MMA and *n*BuA for the synthesis of “MMA-*n*BuA gradient copolymers” is studied as a function of the initial Cu(II) ppm level at a polymerization temperature of 80 °C, considering the reference system defined in Table 1. Next, it is shown that fed-batch procedures are beneficial compared to batch ICAR ATRP under similar overall conditions (e.g., same overall amount of conventional radical initiator). Both single- and multi-component fed batch additions are considered and the relevance of the nature of the conventional radical initiator is highlighted.

3.1. Batch Procedure

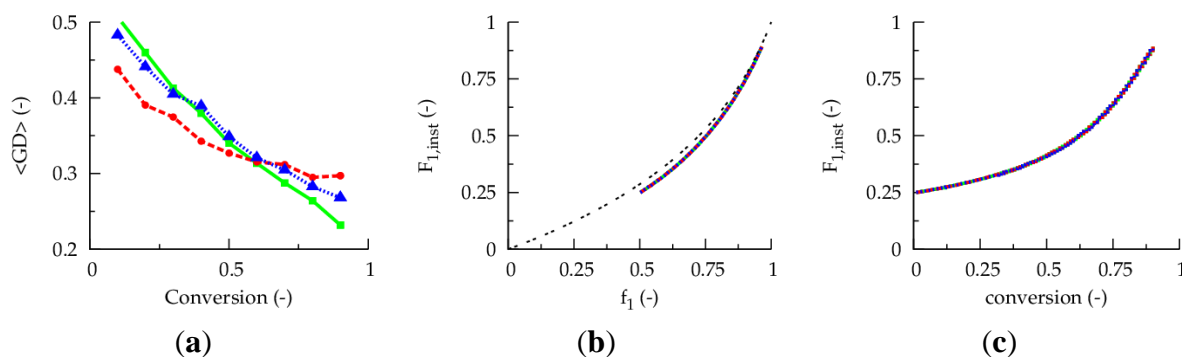
Figure 1a presents the evolution of the gradient deviation ($\langle \text{GD} \rangle$) as a function of conversion for a polymerization temperature of 80 °C, a TCL of 100 and an initial Cu(II) ppm level of 10, 30 and 50 ppm (dashed red, dotted blue and full green line). The selected conventional radical initiator is AIBN and equimolar initial comonomer amounts are applied. Note that such equimolar amounts are selected as conversions leading to almost complete monomer depletion are envisaged for illustration purposes. For a reliable $\langle \text{GD} \rangle$ calculation, the monomer sequences of *ca.* 150,000 copolymer chains are tracked explicitly. It can be seen that the selected ppm level influences the linear gradient quality. Only for the highest ppm level of 50, a $\langle \text{GD} \rangle$ value below 0.25 can be reached at high conversion, implying the necessity of a minimum amount of ATRP catalyst in the reaction medium under batch conditions.

However, as shown in Figure 1b, the initial Cu(II) ppm level has no effect on the evolution of the overall instantaneous copolymer composition ($F_{1,inst}$; monomer 1: *n*BuA) as a function of the feed composition ($f_1 = [M_1]/([M_1] + [M_2])$), *i.e.*, for all growing chains together the incorporation behavior is the same. In agreement with recent simulations of Zapata-González *et al.* [35] in batch CRP, except at low conversions, the well-known Mayo-Lewis behavior is observed for all growing chains (extra black line in Figure 2b; $r_i = k_{p_{ii}}^{chem}/k_{p_{ij}}^{chem}$ ($i \neq j$); r_i : reactivity ratio of monomer i):

$$F_{1,inst} = \frac{r_1 f_1^2 + f_1 f_2}{r_1 f_1^2 + 2 f_1 f_2 + r_2 f_2^2} \quad (1)$$

Hence, based on the different effect of the initial Cu(II) ppm level in Figure 1a,b, it follows that true optimization of radical copolymerization processes requires a thorough understanding of the monomer sequences on the scale of the individual copolymer chains, which is not straightforward based on the Mayo-Lewis equation only. Similarly, for statistical FRP copolymerization involving one functional comonomer in a low overall amount (5 mol%), Ali Parsa *et al.* [36] recently found by means of deterministic and stochastic simulations that half of the polymer chains do not contain this functional comonomer under starved-feed conditions. Importantly, such mismatch between the expected and actual copolymer composition would not be captured by a kinetic model description without an explicit differentiation between polymer chains possessing a given number of functional comonomer units.

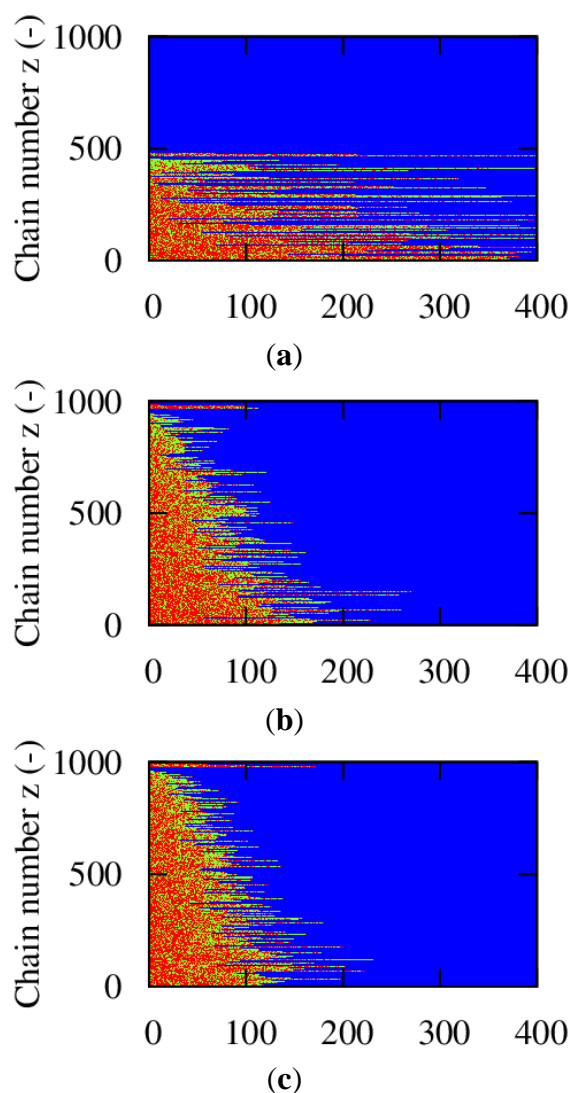
Figure 1. (a) Effect of initial Cu(II) ppm level on the evolution of the gradient deviation ($\langle GD \rangle$) with conversion ($\langle GD \rangle$ of 0.25 needed for high gradient quality). (b) Effect of initial Cu(II) ppm level on the evolution of the overall instantaneous copolymer composition ($F_{1,inst}$) with the feed composition (f_1). (c) Effect of initial Cu(II) ppm level on $F_{1,inst}$ as a function of the conversion; 80 °C; $[M]_0:[R_0X]_0:[I_2]_0 = 100:1:0.02$; $[M_1]_0 = [M_2]_0$; comonomer 1: *n*BuA; comonomer 2: MMA; - - - : 10 ppm; — : 30 ppm; — : 50 ppm; also included in (b) as - - - : Mayo-Lewis equation (Equation (1)); conversion: comonomer 1 + 2; Table 1: intrinsic coefficients.



For a conversion of 0.90, the corresponding explicit monomer sequences are depicted in Figure 2 (red unit: MMA unit; green unit: *n*BuA unit) by selecting randomly a maximum number of 1000 copolymer chains out of the aforementioned 150,000 copolymer chains used for accurate $\langle GD \rangle$ calculation. Less than 1000 copolymer chains result, since incomplete ATRP initiation or termination by recombination can take place leading to the appearance of full horizontal blue dotted lines after the random selection procedure. In addition, in Figure 2, a distinction is made between dormant and dead

polymer chains with the latter type of chains shown in the top region of the polymer sample. Clearly, more well-defined (dormant) gradient copolymer molecules are obtained if a higher initial Cu(II) amount is selected. Higher Cu(II) amounts lead to a smoother transition of one comonomer type into the other comonomer type and to the formation of a higher amount of dormant chains, with additionally a more uniform chain length. Indeed, as confirmed in Figure 3b–d, at high conversion, the lowest dispersity and highest EGF values are obtained in case a ppm level of 50 is used.

Figure 2. Effect of initial Cu(II) ppm level ((a): 10 ppm; (b): 30 ppm; (c): 50 ppm) on the explicit copolymer composition at a conversion of 0.90 (conversion: comonomer 1 + 2); red: MMA unit; green: *n*BuA unit; shown for representative kMC polymer sample (maximum of 1000 out of 150,000 chains); dead polymer chains and dormant polymer chains differentiated (top/bottom region); corresponding average properties (x_n , dispersity, EGF) specified in Figure 3; 80 °C; $[M]_0:[R_0X]_0:[I_2]_0 = 100:1:0.02$; AIBN; $[M_1]_0 = [M_2]_0$; Table 1: intrinsic coefficients.



Unfortunately, at this higher initial Cu(II) ppm level the polymerization rate is much lower, as can be derived from Figure 3a, which shows the effect of the initial Cu(II) ppm level on the conversion

profile. To reach a conversion of 0.90 only 2 h are needed at 10 ppm, whereas already 16 h are required in case 50 ppm is employed. In agreement with previous deterministic simulations on ICAR ATRP homopolymerization [22], too low ppm levels lead to FRP behavior, as a sufficient amount of deactivator is needed to ensure controlled activation-growth-deactivation cycles. For an initial Cu(II) amount of 10 ppm, as shown in Figure 4, the ATRP catalyst is mostly in its activator state and an almost zero deactivator concentration is obtained at high conversion. In contrast, for an initial Cu(II) ppm level of 50, a high amount of ATRP catalyst is always in the deactivator state allowing for control over chain length albeit at the expense of a strong reduction in polymerization rate.

In what follows, it is shown that a fed-batch procedure allows to accelerate the ICAR ATRP process without lowering the control over the copolymer microstructure. A distinction is made between ICAR ATRP processes in which a fed-batch addition procedure is applied for only one compound, namely the conventional radical initiator, and different compounds, *i.e.*, not only the conventional radical initiator but also the comonomers and the deactivator are added in a fed-batch manner.

Figure 3. (a) Conversion as a function of polymerization time. (b) Number average chain length (x_n) as a function of conversion. (c) End-group functionality (EGF) as a function of conversion. (d) Dispersity as a function of conversion; dashed red lines: 10 ppm; blue dotted lines: 30 ppm; full green lines: 50 ppm; 80 °C; $[M]_0:[R_0X]_0:[I_2]_0 = 100:1:0.02$; $[M_1]_0 = [M_2]_0$; conversion: comonomer 1 + 2 ; Table 1: intrinsic coefficients.

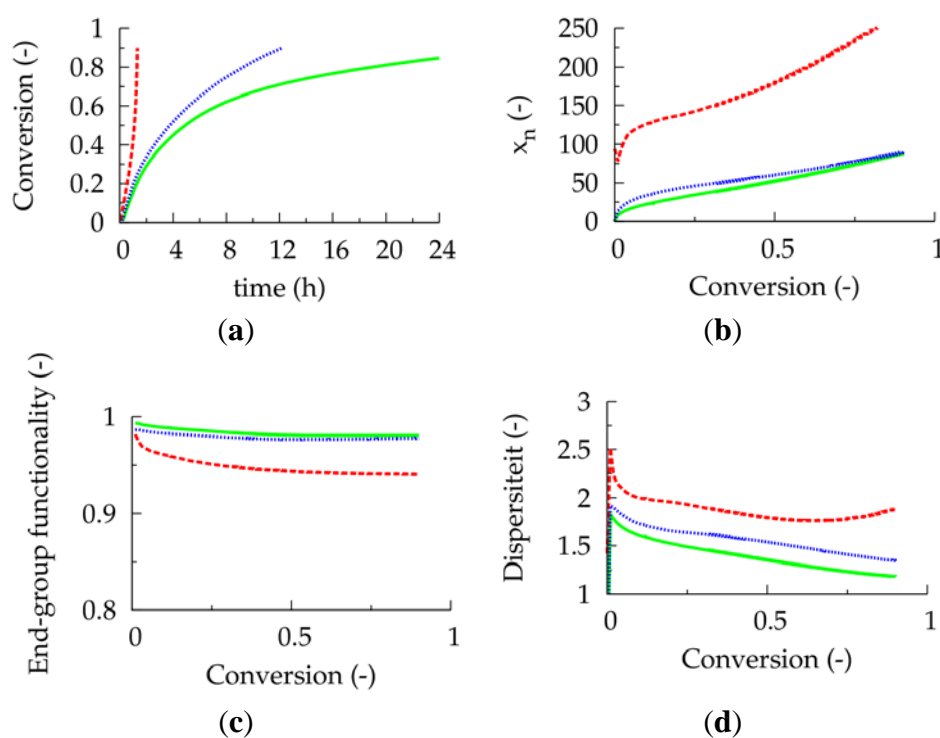
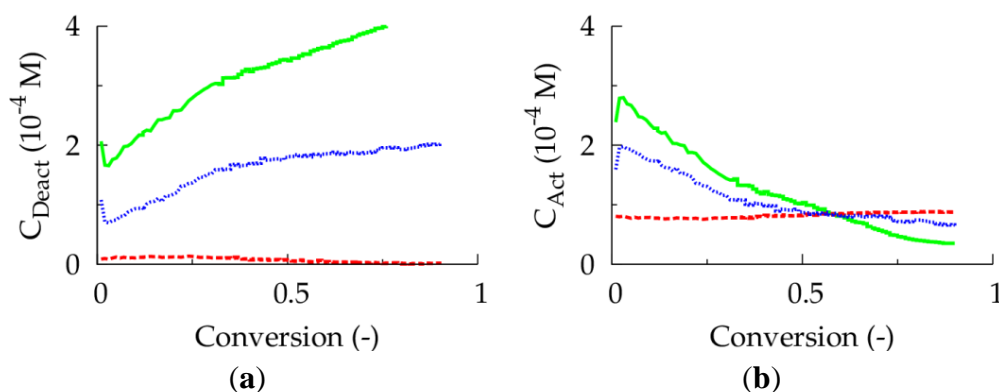


Figure 4. (a) Deactivator concentration as a function of conversion. (b) Activator concentration as a function of conversion; - - - : 10 ppm; — : 30 ppm; — : 50 ppm; 80 °C; $[M]_0:[R_0X]_0:[I_2]_0 = 100:1:0.02$; $[M_1]_0 = [M_2]_0$; Table 1: intrinsic coefficients.



3.2. Fed-Batch Procedure for Addition of Conventional Radical Initiator

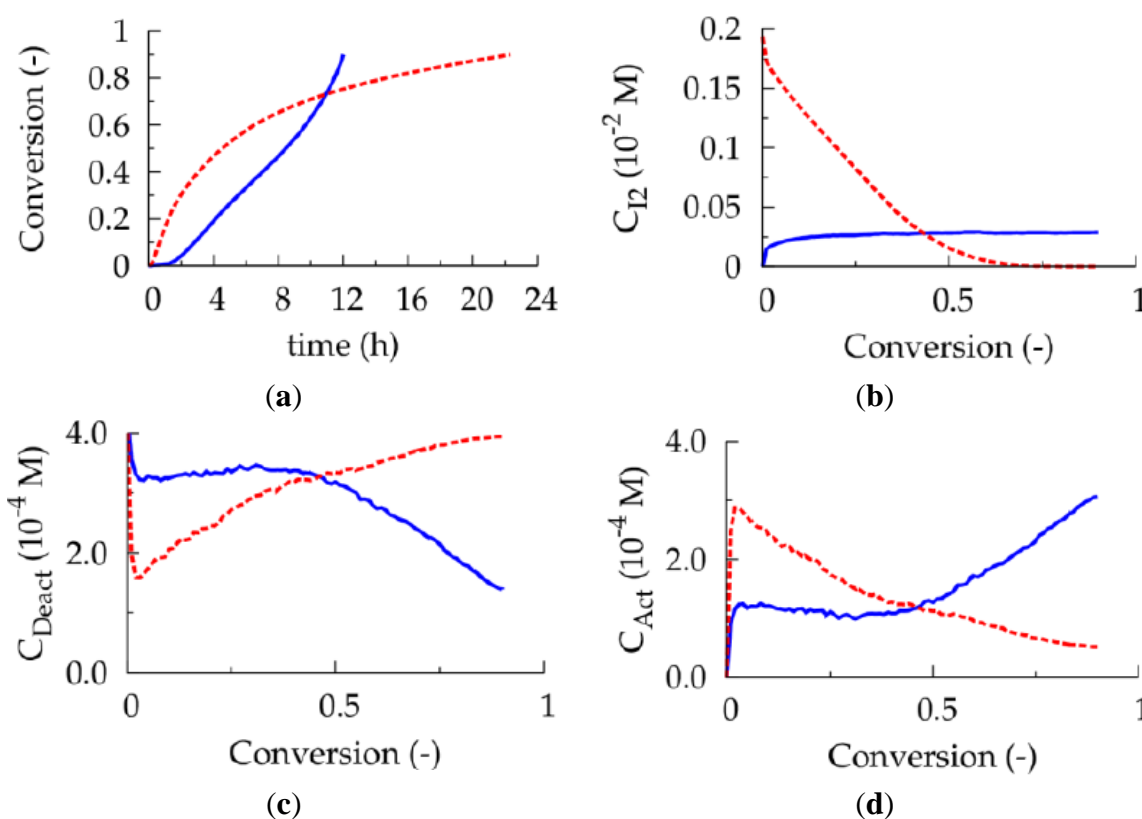
For a successful ICAR ATRP, the conventional radical initiator fragments formed upon dissociation, *i.e.*, the *I* species, should allow for activator generation at the start of the polymerization and for activator regeneration later on in case termination reactions have lowered the radical concentration. Hence, the ideal *I* concentration profile can be calculated *in silico* by (i) starting the polymerization with very little I_2 species, (ii) tracking explicitly the number of termination reactions in the kMC simulations and (iii) “adding” two *I* species each time termination occurs. However, in practice these *I* species have to be created through dissociation of a conventional radical initiator I_2 , which is characterized by a given half-life time. Hence, deviations from this desired concentration profile can be expected, even if a “cocktail” of I_2 species would be used instead.

Based on simulations with this instantaneous “addition” of *I* species, it fortunately follows for example that the continuous addition of a constant low I_2 amount throughout the ICAR ATRP allows to mimic the desired *I* profile. In such simulations, I_2 is added in a dissolved form aiming at low overall change of the volume of the reaction medium ($\ll 1$ vol%). Typical pump flow rates for 1 mL syringes are applied as experimentally applied in literature [37].

For an initial Cu(II) ppm level of 50 aiming at a conversion of 0.90, it is shown in Figure 5a that such alternative fed-batch procedure (full blue lines; 80 °C; TCL = 100; per liter reaction mixture of the corresponding batch case 0.0017 μL dissolved I_2 added per second (concentration of I_2 : 27 $\mu\text{mol L}^{-1}$)) allows for a lowering of the polymerization time compared to the corresponding batch ICAR ATRP. For the sake of comparison, in the batch case the total amount of I_2 added in the fed-batch procedure is present directly at the start of the polymerization (red dashed lines). Note that at low conversion the batch ICAR ATRP process is faster, as a higher conventional radical initiator concentration (Figure 5b; dashed red versus full blue line) is obtained and thus a faster activator (re)generation (Figure 5c,d; red dashed line versus full blue line) takes place. At high conversions, on the other hand, in the fed-batch ICAR ATRP process a higher I_2 concentration results leading to a lowering of the deactivator concentration and a polymerization rate acceleration. The net effect is a lowering of the number of termination events and, hence, a reduction of the overall polymerization time. Importantly, as illustrated in Figure 6 (blue dotted versus red dashed lines), this rate acceleration is not

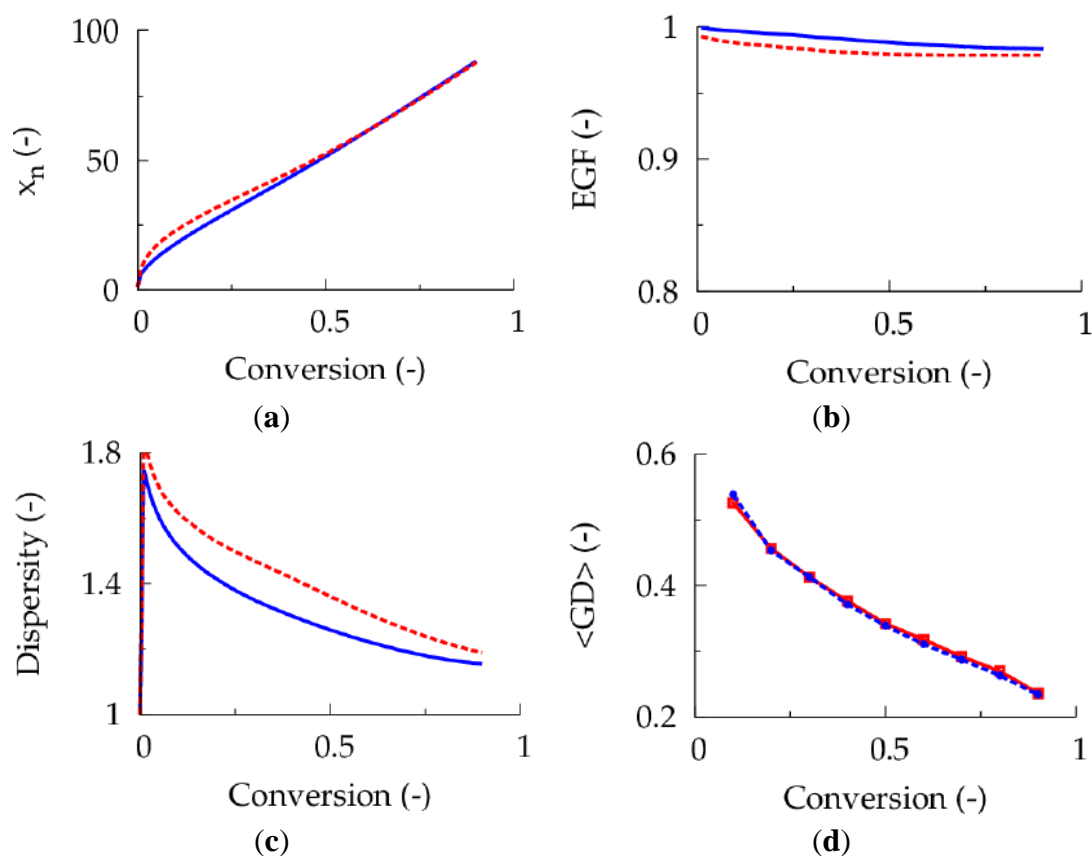
accompanied by a reduction of the control over polymer properties. As for the 50 ppm case, a $\langle\text{GD}\rangle$ value of *ca.* 0.25 now results at high conversion implying a high linear gradient quality.

Figure 5. (a) Conversion as a function of polymerization time. (b) Conventional radical initiator concentration as a function of conversion. (c) Deactivator concentration as a function of conversion. (d) Activator concentration as a function of conversion; common conditions: $[M]_0:[R_0X]_0 = 100:1$, $[M_1]_0 = [M_2]_0$, and 50 ppm Cu(II) initially; - - - : batch $[I_2]_0:[R_0X]_0 = 0.022$ (same amount of I_2 as in fed-batch case up to a conversion of 0.90); — : fed-batch addition of dissolved I_2 : $27 \mu\text{mol}\cdot\text{L}^{-1}$ with flow rate of $0.0017 \mu\text{L s}^{-1}$ per liter reaction mixture of the corresponding batch case; Table 1: intrinsic coefficients.



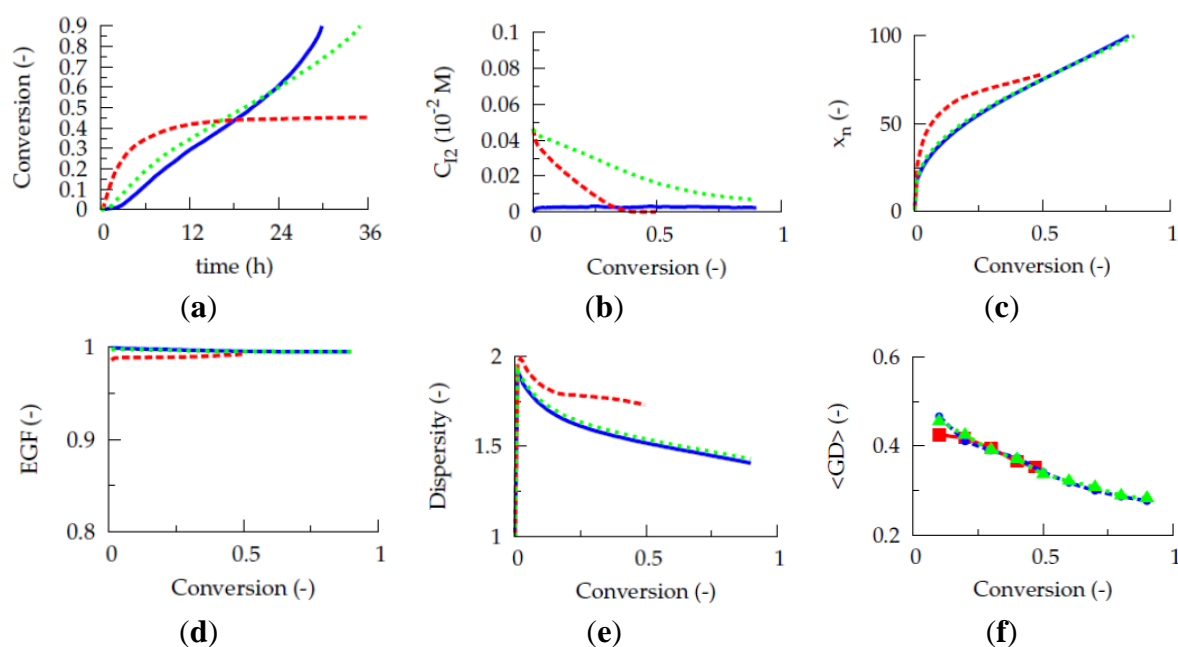
For a lower initial Cu(II) level of 10 ppm (80 °C; TCL = 100), the beneficial effect of a fed-batch approach for the addition of conventional radical initiator is even more pronounced. It follows from Figure 7 that with this fed-batch procedure (full blue vs. dashed red lines), no rate retardation takes place guaranteeing a high conversion while keeping $\langle\text{GD}\rangle$ below 0.30. Note that compared to the 50 ppm case (Figures 5 and 6) less I_2 is added in total ($[I_2]_0:[R_0X]_0 = 0.022$ versus $[I_2]_0:[R_0X]_0 = 0.0052$). As indicated above, to ensure a high control over the ICAR ATRP process FRP behavior has to be circumvented, explaining the lower I_2 amounts in case the initial Cu(II) ppm level is decreased. Such decrease implies, however, a relatively high overall polymerization time (30 h for a conversion of 0.90). Hence, it can be concluded that fed-batch addition of conventional radical initiator allows a more efficient synthesis of ICAR ATRP gradient copolymers in case a sufficiently low feeding rate is selected with respect to the desired Cu ppm level.

Figure 6. (a) Number average chain length (x_n) as a function of conversion. (b) End-group functionality (EGF) as a function of conversion. (c) Dispersity as a function of conversion. (d) Gradient deviation ($\langle \text{GD} \rangle$) as a function of conversion; common conditions: $[M]_0:[R_0X]_0 = 100:1$, $[M_1]_0 = [M_2]_0$, and 50 ppm Cu(II) initially; batch: red dashed line; $[AIBN]_0:[R_0X]_0 = 0.22$ (same amount of I_2 in fed-batch case up to a conversion 0.90); full blue line: fed-batch addition of dissolved I_2 : $27 \mu\text{mol L}^{-1} I_2$ with flow rate of $0.0017 \mu\text{L s}^{-1}$ per liter reaction mixture; Table 1: intrinsic coefficients.



For completeness it is mentioned here that alternatively a conventional radical initiator characterized by a sufficiently high conventional radical initiator half-life time can be used under batch conditions. For example, as illustrated in Figure 7 (green dotted lines; 10 times lower k_{chem} for dissociation than in Table 1), a controlled supply of initiator radicals is then also obtained. Simulations revealed however that the fastest ICAR ATRP is still obtained using the fed-batch approach (blue lines), considering a wide range of half-life times.

Figure 7. (a) Conversion as a function of polymerization. (b) Conventional radical initiator as a function of conversion. (c) Number average chain length (x_n) as a function of conversion. (d) End-group functionality (EGF) as a function of conversion. (e) Dispersity as a function of conversion. (f) Gradient deviation ($\langle GD \rangle$) as a function of conversion; common conditions: $[M]_0:[R_0X]_0 = 100:1$, $[M_1]_0 = [M_2]_0$, and 10 ppm Cu(II) initially; dashed red line: batch $[I_2]_0:[R_0X]_0 = 0.0052$ (same amount of I_2 as overall in fed-batch case up to a conversion of 0.90); full blue line: fed-batch addition of dissolved I_2 : $2.7 \mu\text{mol L}^{-1} I_2$ with flow rate of $0.0017 \mu\text{L s}^{-1}$ per liter reaction mixture of the corresponding batch case; intrinsic rate coefficients: Table 1; dotted green line: conditions as for dashed red line but with ten times lower value for dissociation rate coefficient than specified in Table 1.



3.3. Multi-Component Fed-Batch Procedure for Addition of Conventional Radical Initiator, Comonomer, and Deactivator

In the previous kMC simulations, the total amount of monomer was added completely before the ICAR ATRP was started. Under such conditions, a non-linear relation exists between $F_{1,\text{inst}}$ and the monomer conversion (Figure 1c). However, for a ‘perfect’ linear gradient polymer, it can be expected that a linear relation between $F_{1,\text{inst}}$ and conversion according to the first bisector allows a better control over the monomer sequences toward the targeted linear gradient copolymer microstructure. In practice, the required monomer sequences can be obtained by adjusting in a fed-batch manner the comonomer feed composition through a variation of the added amount of comonomer.

In other words, f_1 should be altered *in situ* so that after each addition $F_{1,\text{inst}}$ is equal to the “overall monomer conversion x_{overall} ”, which is defined with respect to the total amount of monomer used in the corresponding *batch* case:

$$x_{\text{overall}} = \frac{\text{converted amount of nBuA and MMA in fed - batch approach}}{\text{batch amount of nBuA and MMA}} \quad (2)$$

In particular, when the instantaneous overall incorporation of both comonomers is equal ($F_{1,inst} = 0.5$), the “overall conversion” should be 0.5. In practice, the desired f_1 at a given $x_{overall}$ can be obtained based on the Mayo-Lewis equation (Equation (1)) and noting that f_2 is equal to $1-f_1$:

$$x_{overall} = \frac{r_1 f_1^2 + f_1 f_2}{r_1 f_1^2 + 2 f_1 f_2 + r_2 f_2^2} \quad (3)$$

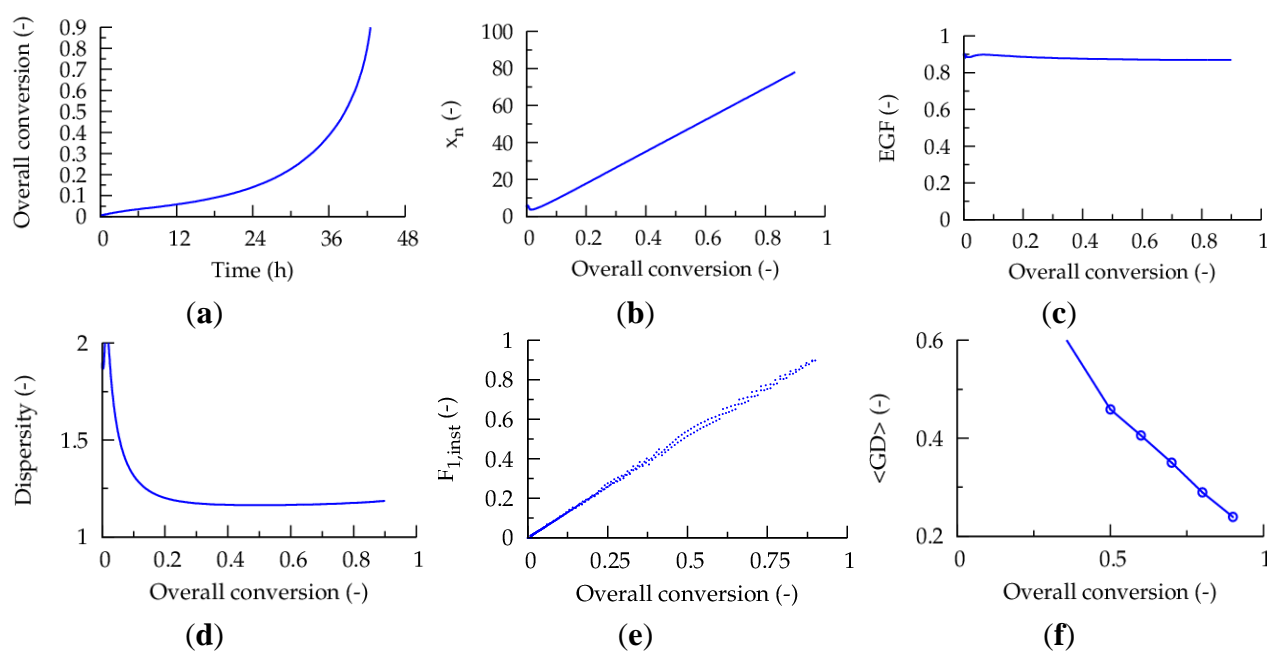
For “normal” ATRP [38] and RAFT polymerization [39], such Mayo-Lewis based fed-batch additions were already explored with computer simulations, while assessing the overall conversion based on the number average chain length, *i.e.*, assuming controlled conditions, and considering a monomer feed policy in which all of the less reactive comonomer is initially present and only the more reactive comonomer is added along the polymerization. However, in these kinetic studies, in which no explicit calculation of the copolymer composition is included, the fed/semi-batch addition of comonomer is accompanied by a low polymerization rate, a rather high dispersity and a relatively low livingness. As indicated in a recent kMC study of Van Steenberge *et al.* [26] low dispersities are required for controlled linear gradient synthesis and it can therefore be expected that under the reported literature conditions still relatively high $\langle GD \rangle$ values are obtained, despite the linear relation between $F_{1,inst}$ and $x_{overall}$.

In this work, the ICAR ATRP fed-batch conditions are carefully selected to minimize the negative tendencies reported for related CRP systems [38,39]. First of all, simulations revealed that it is most suited to start the ICAR ATRP with a low monomer amount and add frequently small amounts of both comonomers under starved-feed conditions, *i.e.*, at a constant high *in situ* conversion (e.g., >0.85) small amounts of both comonomers should be added in order to control the number of monomers added in between a single activation and deactivation. The use of starved-feed conditions is a common procedure in FRP processes with the beneficial safety effect in the case of a sudden loss of cooling capacity [40].

To guarantee a good control over chain length a predefined Cu level is also required taking into account the volume increase of the reaction medium upon fed-batch monomer addition. Hence, deactivator has to be added along the ICAR ATRP process as well. For a direct comparison with the batch condition, it is most suited to add deactivator so that a fixed ppm level of Cu is obtained with respect to the amount of monomer that has been added until the considered time, *i.e.*, calculating the deactivator supply rate based on both the amount of monomer in the monomer feed and the amount of monomer already incorporated in the copolymer chains. In what follows, double quotation marks are used to differentiate such ppm levels from the aforementioned ppm levels. For completeness, it is mentioned here that initially the volume of the ATRP initiator cannot be neglected in these simulations.

In case a high *in situ* monomer conversion of 0.90, *i.e.*, 90% conversion with respect to the cumulative amount of monomer added, is demanded prior to each fed-batch monomer addition, a high gradient quality ($\langle GD \rangle$ of *ca.* 0.20) can be obtained, as illustrated in Figure 8. For these figures, one percentage of the total amount of monomer of the batch counterpart is added initially in pure MMA form and dissolved conventional radical initiator is added continuously (per liter reaction mixture of the corresponding batch case: 0.0017 μL dissolved I_2 added per second (concentration I_2 : 27 $\mu\text{mol L}^{-1}$).

Figure 8. (a) Overall conversion (based on monomer amount of corresponding batch case; Equation (2): as a function of polymerization. (b) Number average chain length (x_n) as a function of overall conversion. (c) End-group functionality (EGF) as a function of overall conversion. (d) Dispersity as a function of overall conversion. (e) Evolution of instantaneous copolymer composition ($F_{1,inst}$) as a function of the overall conversion. (f) Gradient deviation ($\langle GD \rangle$) as a function of conversion; initial conditions: TCL = 100 (in case all monomer would be added instantaneously), and 50 ppm Cu(II); fed-batch addition of dissolved I_2 : $27 \mu\text{mol L}^{-1}$ with flow rate of $0.001 \mu\text{L s}^{-1}$ per liter reaction mixture of the corresponding batch case; fed-batch addition of comonomer based on Equation (3) each time an *in situ* conversion of 0.9 is reached (with at the start 1% of the batch amount in pure MMA form); comonomer addition accompanied by addition of deactivator so that Cu level is again “50 ppm (with respect to the monomer and monomer units)”; Table 1: intrinsic coefficients.

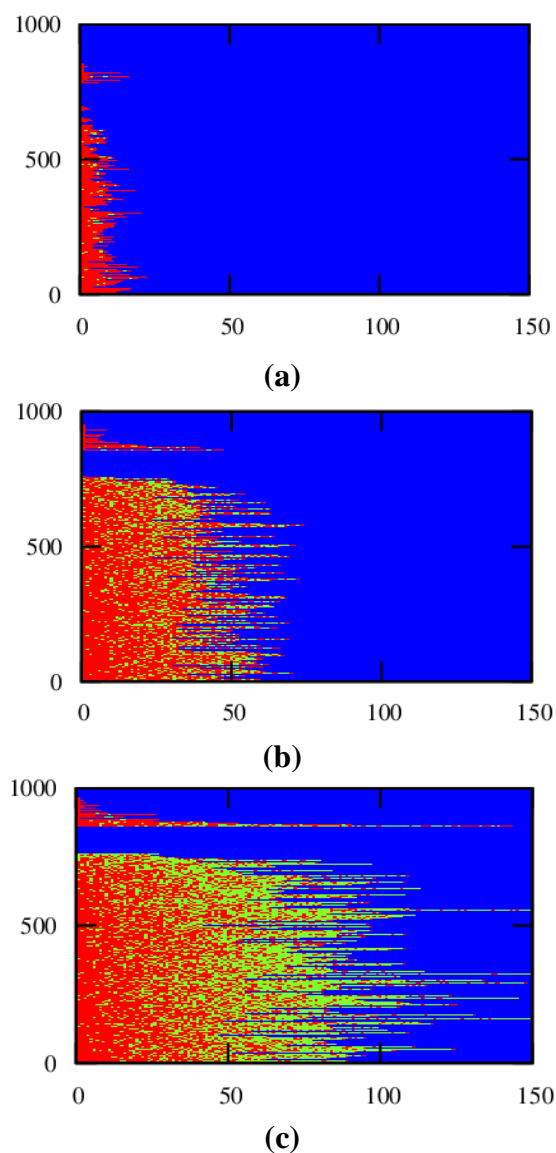


Per addition step, the comonomer molar ratio is adjusted based on Equation (3) so that $F_{1,inst}$ varies linearly with the overall monomer conversion. Furthermore, throughout this ICAR ATRP a Cu level of “50 ppm” is imposed by addition of deactivator each time monomer is added. A total number of *ca.* fifty-five fed-batch additions results, corresponding to an almost negligible drop of the *in situ* monomer conversion upon each monomer addition, implying that the linear gradient microstructure is synthesized via very stable activation-growth-deactivation cycles. Note that the polymerization is conducted already under viscous conditions at low polymerization times, a similar strategy as followed by Bentein *et al.* [41] in their work on the optimization of nitroxide mediated polymerization of styrene.

The high linear gradient quality is confirmed in Figure 9, which shows the corresponding explicit copolymer compositions at an overall conversion of 0.10, 0.50 and 0.90. Importantly, under the studied conditions, at very low overall conversions now almost exclusively MMA (red) units are incorporated, which is a direct consequence of the monomer feed batch policy (Figure 8e versus Figure 1c). Clearly, the dormant copolymer chains possess a much higher linear gradient quality (e.g., Figure 9

versus Figure 2). Note that it can be expected that the oligomeric dead polymer molecules will be washed out upon polymer isolation and thus a polymer product with a very high gradient quality is obtained, underlining the potential of the multi-component fed-batch technique with respect to control over monomer sequences.

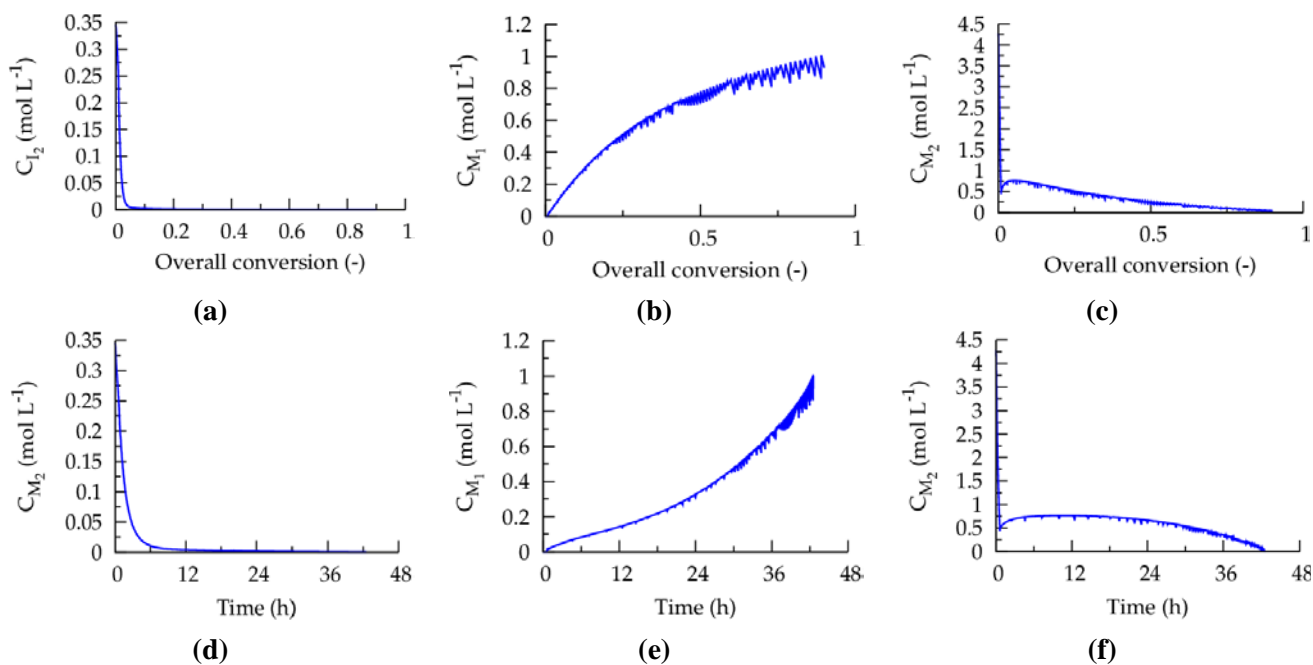
Figure 9. Explicit copolymer composition using multi-component fed-batch procedure at a conversion of (a) 0.10, (b) 0.50 and (c) 0.90; red: MMA unit; green: *n*BuA unit; shown for representative kMC polymer sample; dead polymer chains and dormant polymer chains differentiated (top/bottom region); conditions: see caption of Figure 8; overall conversion: Equation (2): with respect to batch case; Table 1: intrinsic coefficients.



The corresponding evolutions of the comonomer concentrations and concentration of the conventional radical initiator with the overall conversion and polymerization time are given in Figure 10. It can be seen that along the ICAR ATRP the monomer feed is enriched with *n*BuA (monomer 1), as requested for MMA-*n*BuA linear gradient formation. Initially, the conventional radical initiator concentration is high to ensure good activator regeneration. At higher conversions, this concentration drops, due to the

volume increase upon monomer addition, and FRP behavior is thus circumvented leading to a good control over polymer properties. However, despite this excellent control, a relatively slow ICAR ATRP is obtained, in agreement with literature reports on related CRP systems [38,39].

Figure 10. (a) Conventional radical initiator as a function of overall conversion. (b) Comonomer concentrations as a function of overall conversion. (d–f) Corresponding subfigures for (a–c) when expressed as a function of time; conditions: see caption of Figure 8; overall conversion: Equation (2); with respect to batch case; Table 1: intrinsic coefficients.



It can thus be concluded that the highest linear gradient quality can be obtained using a multi-component fed-batch approach, as it allows tailor-design of linear gradient dormant copolymer chains albeit at the expense of an increase of the polymerization time.

4. Conclusions

In silico optimization of isothermal ICAR ATRP of MMA and *n*BuA toward the synthesis of well-defined linear gradient copolymers with low dispersity and high livingness is successfully performed by controlling the monomer sequences of individual copolymer chains.

A fed-batch continuous addition of dissolved conventional radical initiator allows for an increase of the overall polymerization rate compared to the corresponding batch case, considering the same overall amount of conventional radical initiator while aiming at a high conversion and a good control over polymer properties, in case a sufficiently low addition rate is applied. Moreover, for low initial Cu(II) ppm levels, no rate retardation is obtained and a much better control over chain length results compared to the batch case. Alternatively, the batch process can be improved by selecting a conventional radical initiator characterized by a sufficiently high half-life time.

The highest gradient quality for the dormant polymer molecules is obtained if a multi-component fed-batch procedure is selected. In this procedure, not only conventional radical initiator but also

comonomer and deactivator are added in a fed-batch manner under starved-feed conditions. Comonomer is added so that a linear relation between the instantaneous copolymer composition and overall monomer conversion is obtained, considering the Mayo-Lewis equation to calculate the appropriate comonomer feed composition. Per monomer addition, deactivator is added to compensate for the volume increase, *i.e.*, the Cu ppm level is restored *in situ* with respect to the monomer present and the monomer units already incorporated. This procedure, is however, accompanied by a strong reduction of the overall polymerization time compared to the traditional batch operation.

Acknowledgments

The authors acknowledge financial support from the Long Term Structural Methusalem Funding by the Flemish Government, the Interuniversity Attraction Poles Program–Belgian State–Belgian Science Policy, and the Fund for Scientific Research Flanders (FWO; G.0065.13N). Dagmar R. D’hooge acknowledges the Fund for Scientific Research Flanders (FWO) for a (post)doctoral fellowship.

Author Contributions

All authors have contributed to the writing of the results and discussion. D.R.D. and P.H.M.V.S. are responsible for the kinetic Monte Carlo simulations.

Conflicts of Interest

The authors declare no conflict of interest.

References

1. Nicolas, J.; Guillaneuf, Y.; Lefay, C.; Bertin, D.; Gimes, D.; Charleux, B. Nitroxide-mediated polymerization. *Prog. Polym. Sci.* **2013**, *38*, 63–235.
2. Barner-Kowollik, C.; Davis, T.P.; Heuts, J.P.A.; Stenzel, M.H.; Vana, P.; Whittaker, M. RAFTing down under: Tales of missing radicals, fancy architectures, and mysterious holes. *J. Polym. Sci. A Polym. Chem.* **2003**, *41*, 365–375.
3. Matyjaszewski, K.; Xia, J.H. Atom transfer radical polymerization. *Chem. Rev.* **2001**, *101*, 2921–2990.
4. Tsarevsky, N.V.; Matyjaszewski, K. “Green” atom transfer radical polymerization: From process design to preparation of well-defined environmentally friendly polymeric materials. *Chem. Rev.* **2007**, *107*, 2270–2299.
5. Vandenberg, J.; Junkers, T. Synthesis of macromonomers from high-temperature activation of nitroxide mediated polymerization (NMP)-made polyacrylates. *Macromolecules* **2013**, *46*, 3324–3331.
6. Vachaud, M.; D’hooge, D.R.; Socka, M.; Libiszowski, J.; Coulembier, O.; Reyniers, M.F.; Duda, A.; Marin, G.B.; Dubois, P. Inverse dependencies on the polymerization rate in atom transfer radical polymerization of *N*-isopropylacrylamide in aqueous medium. *React. Funct. Polym.* **2013**, *73*, 484–491.

7. Zetterlund, P.B. Compartmentalization effects on bimolecular termination in atom transfer radical polymerization in nanoreactors. *Macromol. Theory Simul.* **2011**, *20*, 660–666.
8. Ghadban, A.; Albertin, L. Synthesis of glycopolymer architectures by reversible-deactivation radical polymerization. *Polymers* **2013**, *5*, 431–526
9. Matyjaszewski, K. Atom transfer radical polymerization: from mechanisms to applications. *Isr. J. Chem.* **2012**, *52*, 206–220.
10. Davis, K.A.; Matyjaszewski, K. Statistical, gradient, block, and graft copolymers by controlled/living radical polymerizations. In *Advances in Polymer Science*, 2nd ed.; Springer-Verlag Berlin Heidelberg: Germany, 2002; pp.1–169.
11. Payne, K.A.; D'hooge, D.R.; Van Steenberge, P.H.M.; Reyniers, M.F.; Cunningham, M.F.; Hutchinson, R.A.; Marin, G.B. ARGET ATRP of butyl methacrylate: utilizing kinetic modeling to understand experimental trends. *Macromolecules* **2013**, *46*, 3828–3840.
12. Nesvadba, P. Radical polymerization in industry. In *Encyclopedia of Radicals in Chemistry, Biology and Materials*; John Wiley & Sons, Ltd.: New York, NJ, USA, 2012.
13. Borguet, Y.P.; Tsarevsky, N.V. Controlled radical polymerization of a styrenic sulfonium monomer and post-polymerization modifications. *Polym. Chem.* **2013**, *4*, 2115–2124.
14. Simakova, A.; Mackenzie, M.; Averick, S.E.; Park, S.; Matyjaszewski, K. Bioinspired iron-based catalyst for atom transfer radical polymerization. *Angew. Chem.* **2013**, *125*, 12370–12373.
15. Fischer, H. The persistent radical effect in controlled radical polymerizations. *J. Polym. Sci. A Polym. Chem.* **1999**, *37*, 1885–1901.
16. Braunecker, W.A.; Matyjaszewski, K. Controlled/living radical polymerization: Features, developments, and perspectives. *Prog. Polym. Sci.* **2007**, *32*, 93–146.
17. Guo, T.; Zhang, L.F.; Pan, X.Q.; Li, X.H.; Cheng, Z.P.; Zhu, X.L. A highly active homogeneous ICAR ATRP of methyl methacrylate using ppm levels of organocopper catalyst. *Polym. Chem.* **2013**, *4*, 3725–3734.
18. Matyjaszewski, K.; Jakubowski, W.; Min, K.; Tang, W.; Huang, J.Y.; Braunecker, W.A.; Tsarevsky, N.V. Diminishing catalyst concentration in atom transfer radical polymerization with reducing agents. *Proc. Natl. Acad. Sci. U.S.A.* **2006**, *103*, 15309–15314.
19. Magenau, A.J.D.; Strandwitz, N.C.; Gennaro, A.; Matyjaszewski, K. Electrochemically mediated atom transfer radical polymerization. *Science* **2011**, *332*, 81–84.
20. Li, X.H.; Wang, W.J.; Li, B.G.; Zhu, S.P. Kinetics and modeling of solution ARGET ATRP of styrene, butyl acrylate, and methyl methacrylate. *Macromol. React. Eng.* **2011**, *5*, 467–478.
21. Konkolewicz, D.; Magenau, A.J.D.; Averick, S.E.; Simakova, A.; He, H.K.; Matyjaszewski, K. ICAR ATRP with ppm Cu catalyst in water. *Macromolecules* **2012**, *45*, 4461–4468.
22. D'hooge, D.R.; Konkolewicz, D.; Reyniers, M.F.; Marin, G.B.; Matyjaszewski, K. Kinetic modeling of ICAR ATRP. *Macromol. Theory Simul.* **2012**, *21*, 52–69.
23. Mukumoto, K.; Li, Y.; Nese, A.; Sheiko, S.S.; Matyjaszewski, K. Synthesis and characterization of molecular bottlebrushes prepared by iron-based ATRP. *Macromolecules* **2012**, *45*, 9243–9294.
24. Toloza Porras, C.; D'hooge, D.R.; Van Steenberge, P.H.M.; Reyniers, M.F.; Marin, G.B. A theoretical exploration of the potential of ICAR ATRP for one- and two-pot synthesis of well-defined diblock copolymers. *Macromol. React. Eng.* **2013**, *7*, 311–326.

25. Hutchinson, R.A.; Penlidis, A. Free-radical Polymerization: Homogeneous Systems. In *Polymer Reaction Engineering*; Asua, J.M., Ed.; Blackwell Publishing Ltd: Oxford, UK, 2008.
26. Van Steenberge, P.H.M.; D'hooge, D.R.; Wang, Y.; Zhong, M.J.; Reyniers, M.F.; Konkolewicz, D.; Matyjaszewski, K.; Marin, G.B. Linear gradient quality of ATRP copolymers. *Macromolecules* **2012**, *45*, 8519–8531.
27. Toloza Porras, C.; D'hooge, D.R.; Van Steenberge, P.H.M.; Reyniers, M.F.; Marin, G.B. Design of ICAR ATRP toward estimation of intrinsic macro-activation/deactivation Arrhenius parameters under polymerization conditions. *Ind. Eng. Chem. Res.* **2014**, submitted.
28. Johnston-Hall, G.; Stenzel, M.H.; Davis, T.P.; Barner-Kowollik, C.; Monteiro, M.J. Chain length dependent termination rate coefficients of methyl methacrylate (MMA) in the gel regime: Accessing k_t^{ij} using reversible addition-fragmentation chain transfer (RAFT) polymerization. *Macromolecules* **2007**, *40*, 2730–2736.
29. Johnston-Hall, G.; Monteiro, M.J. Bimolecular radical termination: New perspectives and insights. *J. Polym. Sci. A Polym. Chem.* **2008**, *46*, 3155–3173.
30. D'hooge, D.R.; Reyniers, M.F.; Marin, G.B. The crucial role of diffusional limitations in controlled radical polymerization. *Macromol. React. Eng.* **2013**, *7*, 362–379.
31. Akzonobel. Available online: <http://www.akzonobel.com> (accessed on 4 February 2014).
32. Van Steenberge, P.H.M.; Vandenberg, J.; D'hooge, D.R.; Reyniers, M.F.; Adriaensens, P.J.; Lutsen, L.; Vanderzande, D.J.M.; Marin, G.B. Kinetic monte carlo modeling of the sulfinyl precursor route for Poly(p-phenylene vinylene) synthesis. *Macromolecules* **2011**, *44*, 8716–8726.
33. Van Steenberge, P.H.M.; D'hooge, D.R.; Vandenberg, J.; Reyniers, M.-F.; Adriaensens, P.J.; Vanderzande, D.J.M.; Marin, G.B. Kinetic Monte Carlo modeling of the sulfinyl precursor route for poly(para-phenylene vinylene) synthesis. *Macromol. Theory Simul.* **2013**, *22*, 246–255.
34. Van Steenberge, P.H.M.; D'hooge, D.R.; Reyniers, M.F.; Marin, G.B. Improved kinetic Monte Carlo simulation of chemical composition-chain length distributions in polymerization processes. *Chem. Eng. Sci.* **2014**, *110*, 185–199.
35. Zapata-González, I.; Hutchinson, R.A.; Matyjaszewski, K.; Saldívar-Guerra, E.; Ortiz-Cisneros, J.; Copolymer composition deviations from Mayo-Lewis conventional free radical behavior in nitroxide mediated copolymerization. *Macromol. Theory Simul.* **2014**, in press.
36. Parsa, M.A.; Kozhan, I.; Wulkow, M.; Hutchinson, R.A. Modeling of functional group distribution in copolymerization: A comparison of deterministic and stochastic approaches. *Macromol. Theory Simul.* **2014**, in press.
37. Vandenberg, J.; Junkers, T. Use of a Continuous-flow microreactor for thiol-ene functionalization of RAFT-derived poly(butyl acrylate). *Polym. Chem.* **2012**, *3*, 2739–2742.
38. Wang, R.; Luo, Y.; Li, B.G.; Zhu, S. Control of gradient copolymer composition in ATRP using semibatch feeding policy. *AIChE J.* **2007**, *53*, 174–186.
39. Wang, R.; Luo, Y.; Li, B.G.; Zhu, S. Design and control of copolymer composition distribution in living radical polymerization using semi-batch feeding policies: A model simulation. *Macromol. Theory Simul.* **2006**, *15*, 336–368.
40. Wang, W.; Hutchinson, R.A. Recent advances in the study of high-temperature free radical acrylic solution copolymerization. *Macromol. React. Eng.* **2008**, *2*, 199–214.

41. Bentein, L.; D'hooge, D.R.; Reyniers, M.F.; Marin, G.B. Kinetic modeling as a tool to understand and improve the nitroxide mediated polymerization of styrene. *Macromol. Theory Simul.* **2011**, *20*, 336–368.

© 2014 by the authors; licensee MDPI, Basel, Switzerland. This article is an open access article distributed under the terms and conditions of the Creative Commons Attribution license (<http://creativecommons.org/licenses/by/3.0/>).